

Experimental Result of ${}^3\text{He}({}^3\text{He},2\text{p}){}^4\text{He}$ Reaction in OCEAN

M. Komori,^{a,b} T. Itahashi,^a N. Kudomi,^a K. Kume,^a K. Takahisa,^a S. Yoshida,^a H. Ejiri,^a
H. Ohsumi,^c H. Toki,^a and Y. Nagai^a

^aResearch Center for Nuclear Physics (RCNP), Ibaraki, Osaka 567-0047, Japan

^bNational Institute of Radiological Sciences (NIRS), Chiba 263-8555, Japan

^cDept. of Culture and Education, Saga Univ., Saga 840-8502, Japan

The experimental result in OCEAN measurement of the solar nuclear ${}^3\text{He}({}^3\text{He},2\text{p}){}^4\text{He}$ reaction at the energy of 30 to 45 keV is reported. The ${}^3\text{He}^{2+}$ beam of $100\mu\text{A}$ and a windowless gas target with a differential pumping system were used. In order to detect the reaction particles by the reaction, $\Delta\text{E-E}$ counter telescope was placed in the gas target. At the same time, the beam acceleration voltage, the beam intensity, the target gas pressure and the target gas temperature were measured[1].

The cross sections for every reaction energy are driven by the following analysis procedure. The number of counts $dN(z)$ per unit of time arising from a differential length dz of extended ${}^3\text{He}$ gas target is given by the expression

$$dN(z) = N_t \cdot N_b \cdot \sigma(E(z)) \cdot \eta(z) \cdot dz, \quad (1)$$

where $N(z)$ is the number of counts for ${}^3\text{He}+{}^3\text{He}$ reaction, N_t is the target density, N_b is the beam intensity per unit of time and $\eta(z)$ is the absolute detection efficiency. For the case of a thin target, introducing an effective reaction energy E_{eff} corresponding to the mean value of the projectile energy distribution in the detection setup, the stopping power ϵ (i.e. the energy loss per unit length) and integrating for the full target length, one arrives at

$$N = N_t \cdot N_b \cdot \sigma(E_{\text{eff}}) \cdot \int_L \eta(E) \cdot \epsilon(E)^{-1} \cdot dE. \quad (2)$$

For evaluation of the cross section, the number of counts for the ${}^3\text{He}+{}^3\text{He}$ reaction, the target density and the beam intensity are driven from the measured value. The values for the effective reaction energy and the integral term for detection efficiency were derived from the Monte Carlo program of SRIM and GEANT3. The number of counts for the ${}^3\text{He}+{}^3\text{He}$ reaction are driven from the acceptable area in the measured $\Delta\text{E-E}$ scatter plot.

The area should be determined considering the signal-to-noise ratio(S/N). The origin of the background(Noise) events are assumed to be ${}^3\text{He}+d$ reaction as well as the cosmic rays and the electrical noise. The energy distribution of ΔE (0~10 MeV)-E (0~16 MeV) counter telescope is divided into 16000 of $100\text{ keV} \times 100\text{ keV}$ parts as shown in Fig. 1. For every part, S/N ratio is allotted and the parts which had better S/N ratio, are adopted for the acceptable area for the ${}^3\text{He}+{}^3\text{He}$ events. The distribution of ${}^3\text{He}+{}^3\text{He}$ (Signal) events in the scatter plot was simulated by the Monte Carlo program. Also, the distribution of the ${}^3\text{He}+d$ events was simulated considering the deuterium contamination in the target gas derived from the accepted events as the ${}^3\text{He}+d$ reaction in $\Delta\text{E-E}$ scatter plot. The allocation of other background components

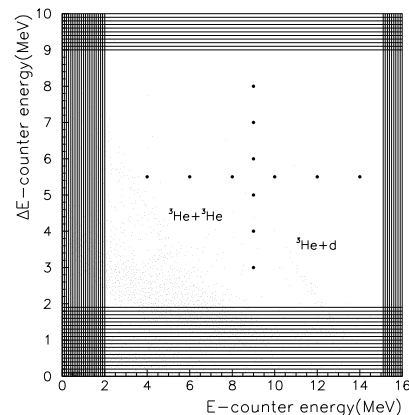


Figure 1: $\Delta\text{E-E}$ scatter plot.

was obtained by the experimental background measurements. These background events are normalized by the real time of the ${}^3\text{He}+{}^3\text{He}$ reaction measurements. After the S/N ratio is estimated for every part of $100\text{ keV} \times 100\text{ keV}$, all parts are ordered again as a function of the S/N ratio to determine the acceptable area for the ${}^3\text{He}+{}^3\text{He}$ events.

Fig. 2(a) shows the distribution of the simulated ${}^3\text{He}+{}^3\text{He}$ reaction as the function of the S/N ratio. Many of the events are located in the right hand side in Fig. 2(a), corresponding to the better S/N ratio. Also, Fig. 2(b) and (c) show the distributions of the simulated ${}^3\text{He}+d$ reaction events and the observed other background events normalized as discussed above. These background events are located in the left hand side in each figures. Fig. 2(d) shows the distribution of the observed ${}^3\text{He}+{}^3\text{He}$ events at $E_{\text{cm}}=45\text{ keV}$, as the function of the S/N ratio. In such an energy region, the contributions from these background events are very small. Therefore the observed distribution of the ${}^3\text{He}+{}^3\text{He}$ reaction is similar to the simulated one without any background subtractions. From these analysis, most of the background events are found to be located in less than 13000 channel.

Therefore, the acceptable area for the ${}^3\text{He}+{}^3\text{He}$ reaction are determined over 13000 channel.

The resulting $S(E)$ values from this work as well as previous data from Dwarakanath (1971) [2], Krauss (1987) [3] and LUNA (1998) [4] are shown in Fig. 3. The obtained data are in a good agreement with the result of Krauss(1987), and they appear to be larger as the reaction energy is smaller. The statistical error of the present measurement at $E_{\text{cm}}=45.3\text{ keV}$ is 1.7%, which is better than that of Krauss(1987). As a result, the present experiment with OCEAN has proved to be more powerful compared to the other existing facilities, since it realized to deliver over 1 mA for ${}^3\text{He}^{1+}$ beam and $100\text{ }\mu\text{A}$ for ${}^3\text{He}^{1+}$ beam. Consequently, we can expect that the total event more than 100 counts in the energy range from 20 to 25 keV, could be obtained for a running time of about one month. Owing to OCEAN which provide not only singly charged but also doubly charged ${}^3\text{He}$ beam, one can continuously study wide region between 20 to 50 keV center of mass energy, which is not accessible for LUNA facility. It is important to investigate the enhancement for the ${}^3\text{He}({}^3\text{He},2p){}^4\text{He}$ reaction due to the electron screening effects which will become manifest in the low energy region.

References

- [1] T. Itahashi, *etal.*, Rev. Sci. Instrum. **69** (1998) 1032.
- [2] M.R. Dwarakanath and H. Winkler, Phys. Rev. **C4** (1971) 1532.
- [3] A. Krauss, *etal.*, Nucl. Phys. **A467** (1987) 273.
- [4] M. Junker, *etal.* (LUNA Collaboration), Phys. Rev. **C57** (1998) 2700.

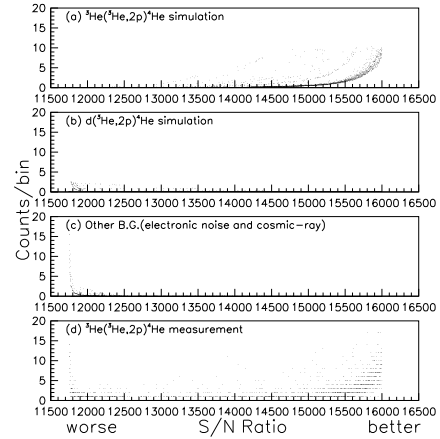


Figure 2: Event distribution ordered as the S/N ratio.

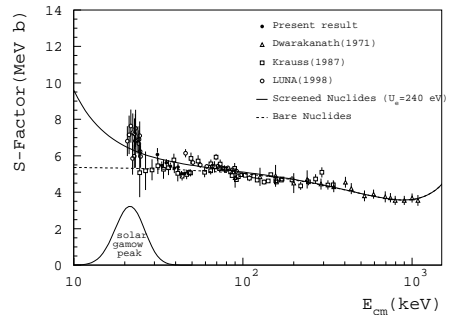


Figure 3: Astrophysical S-factor.